Int. J. Electrochem. Sci., 17 **(2022)** Article Number: 221256, doi: 10.20964/2022.12.56

International Journal of
ELECTROCHEMICAL
SCIENCE
www.electrochemsci.org

Short Communication

Preliminary Investigation on Application of VO_2, Polyaniline, and Ethanolic Extracts of Different Fruits as Components for DSSCs

A. R. Gomes, L. A. T. Costa, M. P. A. Silva, N. S. R. Tomé, D.T. Cestarolli and E. M. Guerra[*]

Departamento de Química, Biotecnologia e Engenharia de Bioprocessos, Universidade Federal de São João Del Rei – Campus Alto Paraopeba, Rod. MG 443, Km 07, CEP 36420-000, Ouro Branco, MG, Brazil
[*]E-mail: elidiaguerra@ufsj.edu.br

Received: 13 October 2021 / *Accepted:* 21 November 2022 / *Published:* 27 December 2022

The energy levels of dye-sensitized solar cells (DSSCs) using a combination of vanadium dioxide (VO_2), polyaniline (PANI), and dyes such as blueberries (*Vaccinium myrtillus*), blackberries (*Morus nigra*), beetroots (*Beta vulgaris*), jabuticaba wine, and strawberries (*Fragaria sp*, were evaluated. UV-visible absorption spectroscopy, cyclic voltammetry, and Tauc's method were used to study the energy levels of the dyes, VO_2, and PANI. The energy levels of PANI varied during the electrodeposition of the monomer in different reaction media and concentrations. The results showed that VO_2 has potential applications as anode material in DSSCs. In addition, the energy parameters of different dyes and different solutions of PANI make it possible to assemble 24 combinations of DSSCs.

Keywords: solar cell, DSSC, VO_2, PANI, solar dyes

1. INTRODUCTION

Finding a renewable, sustainable, and low-cost energy solution has been a popular objective of current research. One of the key objectives in solar cell research is finding alternatives to the increasingly scarce and expensive active materials and semiconductors used in solar cells. These devices convert sunlight into electrical energy [1]. Basically, the concept of its functioning is explained by the excitation of electrons from solar irradiation and captured at the anode. From this point, the electron is injected with energy below of Fermi level from the cathode into the cell and is used to do work as electrically or voltage times current. The sequence of electron injection of solar cell is showed in Figure 1.

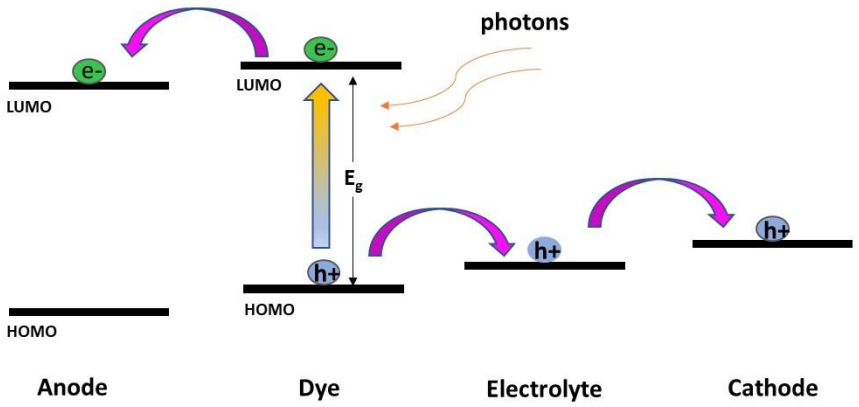

Figure 1. Scheme of an energy level diagram for a solar cell.

From sunlight, a photon is absorbed by the photoactive material, also known as the donor (the dye in this example). This excites the electron of the highest occupied molecular orbital (HOMO) into the lowest unoccupied molecular orbital (LUMO), generating an electron-hole pair known as an exciton. The exciton reaches the donor/acceptor interface, favoring electron transfer from the LUMO of the donor to the LUMO of the acceptor (the anode in this example) [2]. The electron is transported through the anodic electrode interface, while the hole left in the HOMO of the donor is transported through the electrolyte (or hole-transport material) to the cathodic electrode. In the case of a dye-sensitizer solar cell (DSSC), the mechanism of electron transfer is initiated by the photoexcitation of dye molecules that are adsorbed onto the material of the anodic electrode, typically a semiconductor metal oxide such as vanadium dioxide (VO_2). VO_2 is a semiconductor at room temperature, but has a phase transition temperature of T_c = 68 °C, where it changes from a semiconductor to a metal [3–5]. In addition, VO_2 exhibits a bolometric effect, which is a characteristic of a reduction in electrical resistance by four orders of magnitude over a small temperature range when the change from semiconductor to metal occurs [3,6–9]. Polyaniline (PANI) is a well-known electron donor material that can result in improved power conversion efficiency (PCE) [10–13]. Tauc's method of optical band gap determination can be used to evaluate the suitability of both VO_2 and PANI for use in solar cells [14]. The band gap is determined using Equation (1):

$$\alpha h\nu^n = B(h\nu - E_{gap}) \quad (1)$$

where α is the absorption coefficient, h is Planck's constant, ν is the photon frequency, E_{gap} is the band gap, and B is the slope of the linear portion of the Tauc plot [15,16]. The index n represents the transition energy gap. The plot of $(\alpha h\nu)^2$ versus hν is a linear function of the direct allowed band transition in the samples. Extrapolating the linear dependence of the relation to the abscissa yields the corresponding direct allowed band gap [13,17]. Our interest is to investigate the combination of materials such as VO_2, PANI, and different dyes as components in DSSCs, as well as their LUMO, HOMO, and band gap energies.

2. EXPERIMENTAL

2.1. Synthesis of VO_2

Powdered V_2O_5 (0.2 g) in distilled water (50 mL) was sonicated for 30 min. Citric acid monohydrate (1.4 mmol) was added with constant stirring and heated at 75 °C for 1 h.). The mixture was placed in an autoclave at 200 °C for 12 h and cooled at room temperature to complete the hydrothermal synthesis. The VO_2 obtained was deposited on an ITO/PET support by casting and drying at room temperature. The mass and area of the VO_2 were controlled.

2.2. Synthesis by electrodeposition of PANI

PANI was synthesized by *in situ* electrochemical polymerization oxidation, from its monomer, on PET/ITO substrates [32]. Initially, the monomer was purified by vacuum distillation to remove the oxidized species. An electrochemical cell was employed. The electrochemical cell used PET/ITO as the working electrode, a Pt wire as the counter electrode, Ag/AgCl as the reference electrode, and a solution containing different concentrations of aniline and electrolyte solutions, as described in Table 1.

Table 1. Concentrations of aniline and solutions for polyaniline synthesis.

Electrolyte	Name	Aniline (mol/L)	Solution (mol/L)
Condition 1	C1	0.3	0.5 of H_2SO_4
Condition 2	C2	0.05	0.1 of H_2SO_4
Condition 3	C3	0.05	0.25 of $HClO_4$ in 5 ml of ACN
Condition 4	C4	0.5	1.0 of H_2SO_4
Condition 5	C5	0.1	0.1 of $H_2C_2O_4$
Condition 6	C6	0.25	1.0 of H_2SO_4

2.3. Extraction of dyes from fruits

We chose to study dyes that were phenolic compounds, as they can bind to the metal oxide layer through the phenolic group and are able to strongly absorb solar radiation in the visible region [29]. Therefore, blueberries (*Vaccinium myrtillus*), blackberries (*Morus nigra*), beetroots (*Beta vulgaris*), jabuticaba wine, and strawberries (*Fragaria sp.*) were chosen as dyes. The extracts were obtained according to literature procedures [12]. The fruits were macerated (with mortar and pestle or by heating), its dyes were extracted by mixing with ethanol and filtering and subsequently stored in a refrigerator.

The ratio of solid material to solvent was 1:3 by mass [12,25]. For the beetroot extract, it was necessary to cut the beetroot into small pieces, add ethanol at a ratio of 1:2 (m/m) solid to solvent, and leave the mixture to rest for 48 h prior to filtration [22,25]. Electrochemical studies were carried out using dyes adhered to the working electrode, with Ag/AgCl as the reference electrode, Pt as the counter electrode and $LiClO_4$ in acetonitrile (0.1 mol·L^{-1}) as the electrolyte solution.

Using the chronoamperometry technique, PANI films were electrodeposited on the surface of the PET/ITO. Electrochemical experiments were performed on a potentiostat/galvanostat μ-AutoLab III interfaced to a computer using a NOVA 2.0 software. Electronic absorption spectra were measured using a UV-Vis spectrophotometer UV3600, Shimadzu. The absorption data is taken from 300 nm to 800 nm wavelength. A 10 mm quartz was used for the samples. The results extracted from analyzes were made using the direct transition. The direct energy gap was calculated using UV-Vis spectra and the Tauc relation (Eq. 1). Additionally, the frontier orbitals (HOMO and LUMO) were estimated using Equations 2 and 3 [16]:

$$E_{HOMO} = -(E_{ox}^{onset} + 4.99) \quad (2)$$

$$E_{LUMO} = E_{HOMO} + E_{gap} \quad (3)$$

3. RESULTS AND DISCUSSION

3.1. Energies of PANI electrodeposited in different conditions

Figure 2 shows the UV-Vis absorption spectra of PANI obtained via electrodeposition using different concentrations and types of electrolytes.

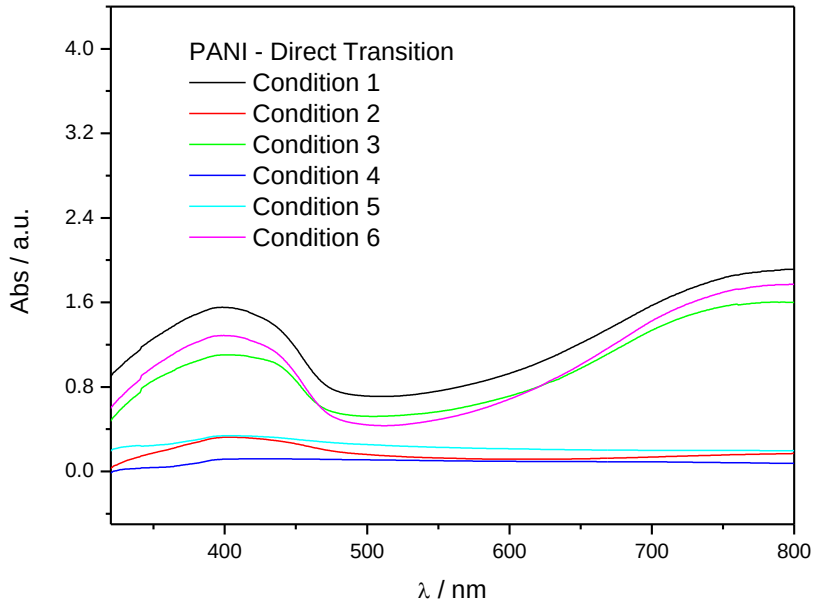

Figure 2. UV-Vis spectra of PANI electrodeposited using different concentrations and types of electroyte solutions.

PANI in its emerald form has an absorption band in the visible region, which is attributed to the π–π* electronic transition of the conjugated polymer. The absorption bands observed near 400 nm are attributed to the electronic transition of the HOMO of the benzenoid ring to the LUMO of the quinoid ring [18]. The UV-Vis spectra for PANI synthesized from conditions 2, 4 and 5 (Table 1) have weak absorption across the entire visible spectral region. It is necessary for materials to have the largest possible absorption in the visible region of the spectrum for applications in solar cells, because cell performance depends on the generation of electron-hole pairs caused by absorption in the visible spectrum [18], as in condition 1 (C1).

For a solar cell, it is essential to know the difference in energy between the valence and conduction bands of the materials, known as the band gap, that will be used in its construction. It was possible to estimate the band gap of each material through electronic spectroscopy in the UV-Vis region by utilizing the Tauc plot method. Table 2 lists the band gap values measured for each sample using the Tauc plot method. The HOMO energy levels were calculated using the oxidation values obtained from cyclic voltammetry (Eq. 2), which are listed in Table 3. The LUMO energy levels were estimated using Equation 3 [16].

Table 2. Band gap values estimate for PANI electrodeposited using different concentrations and types of electrolyte solutions.

PANI in different concentrations of monomer in acid medium	**E_{gap} (eV)**
C1	2.52
C2	2.40
C3	2.57
C4	2.34
C5	1.54
C6	2.55

During the study of the band gap, it is noticed that it is generally related to the wavelengths and their absorptions. The largest band gap is related to absorption at shorter wavelengths, as occurred in C3, while the lowest band gap, found in C5, is related to absorption at longer wavelengths.

Table 3. Anodic peak potentials of PANI electrodeposited using different concentrations and types of electrolyte solutions.

Compounds	**E_{ox} (V) *vs* Ag/AgCl**
C1	-1.07
C2	-0.59
C3	-1.30
C4	-1.10
C5	-0.56
C6	-1.04

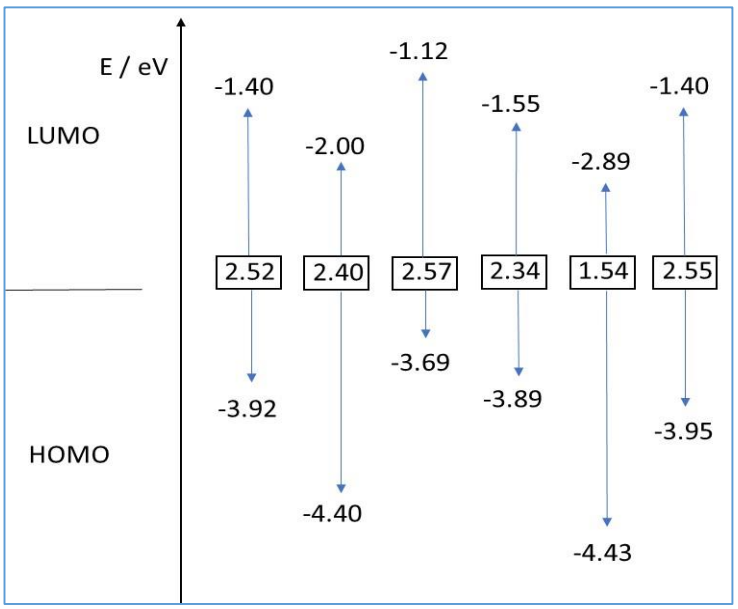

Figure 3. Diagram of the energy bands of PANI electrodeposited using different concentrations and types of electrolyte solutions (C1 to C6, being left to right).

3.2. Energies of VO_2

The UV-Vis spectrum of VO_2 is shown in Figure 4. An intense absorption onset band with a maximum at approximately 448 nm was observed, which was assigned to the d–d transitions of V(4+) ions as well oxygen (O) to vanadium (V) charge transfer in an octahedral coordination [4].

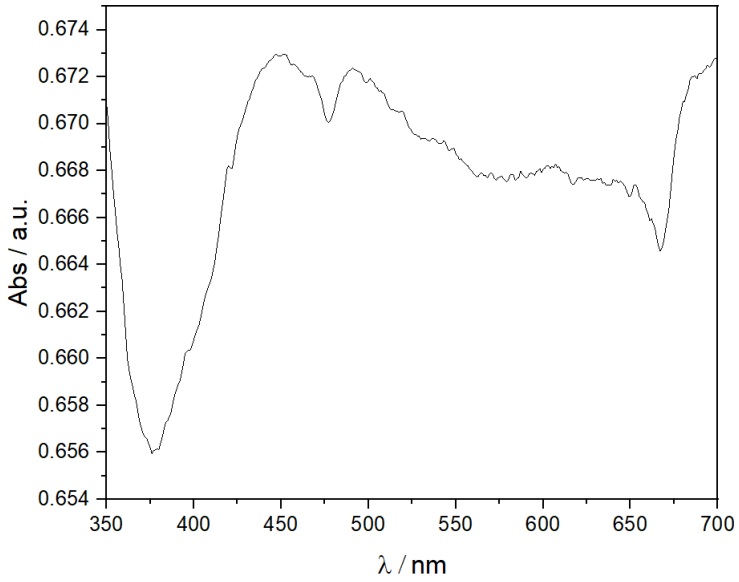

Figure 4. UV-Vis spectrum of VO_2.

Using the Tauc plot of the UV-Vis spectrum the E_{gap} was estimated as 3.02 eV. From the cyclic voltammogram of VO_2 (Figure 5) the anodic peak (E_{ox}) was measured at 1.2 V (vs Ag/AgCl). These values were used with Equations 2 and 3 to estimate the HOMO and LUMO energy levels, which are shown in Figure 6.

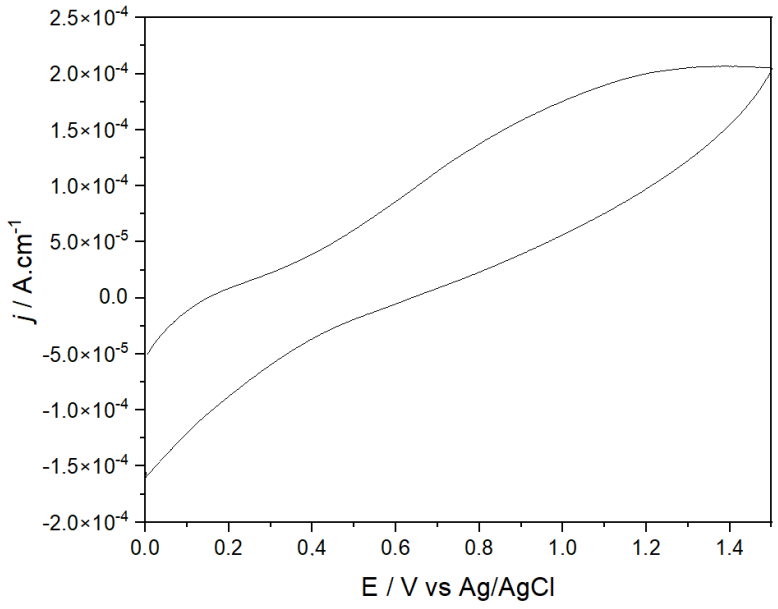

Figure 5. Cyclic voltammogram of VO_2.

Then, from these Equations 2 and 3 were obtained the values E_{gap} = 3.02 eV, HOMO = -6.19V and LUMO = -3.17 eV as showed in Figure 6:

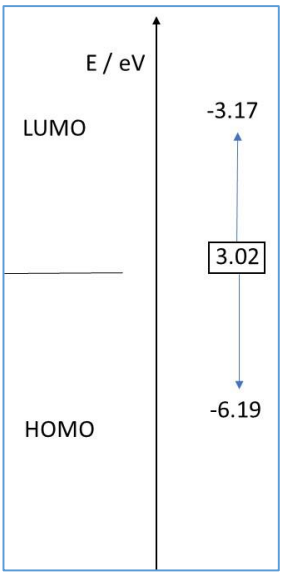

Figure 6. Diagram of the energy bands of VO_2.

3.3. Energies of dyes

The electronic absorption spectra of the extracted dyes are shown in Figure 7. The extracted dyes showed strong absorbance in the 470–550 nm range. Anthocyanins are known to exhibit absorbance peaks around 530 nm [18], indicating that the dye extracts mainly contain anthocyanins.

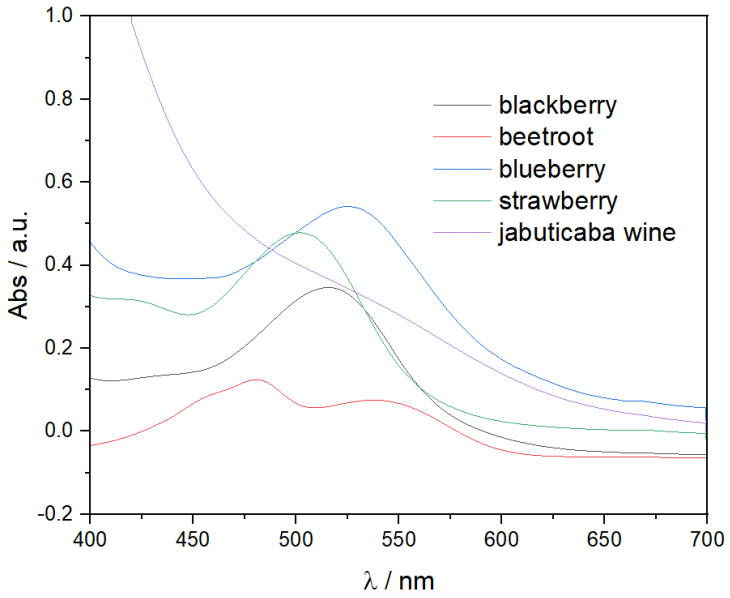

Figure 7. UV-vis spectrum of ethanolic extracts of dyes.

The visible bands are assigned to π–π* charge transfers, which result in a shift of the electronic charge density from the chromium part to the catechol part of the anthocyanin molecules [19]. The

wavelength of 520 nm is the wavelength of the cyanidin moiety [18]. Using the Tauc plot, it was possible to estimate the energy of the band gaps of the different dyes, as shown in Table 3.

From cyclic voltammograms (Figure 8), the anodic peak potentials of the ethanolic extract for each dye were obtained (Table 4). Equations 2 and 3 were used to estimate the HOMO and LUMO energy levels as shown in Figure 9.

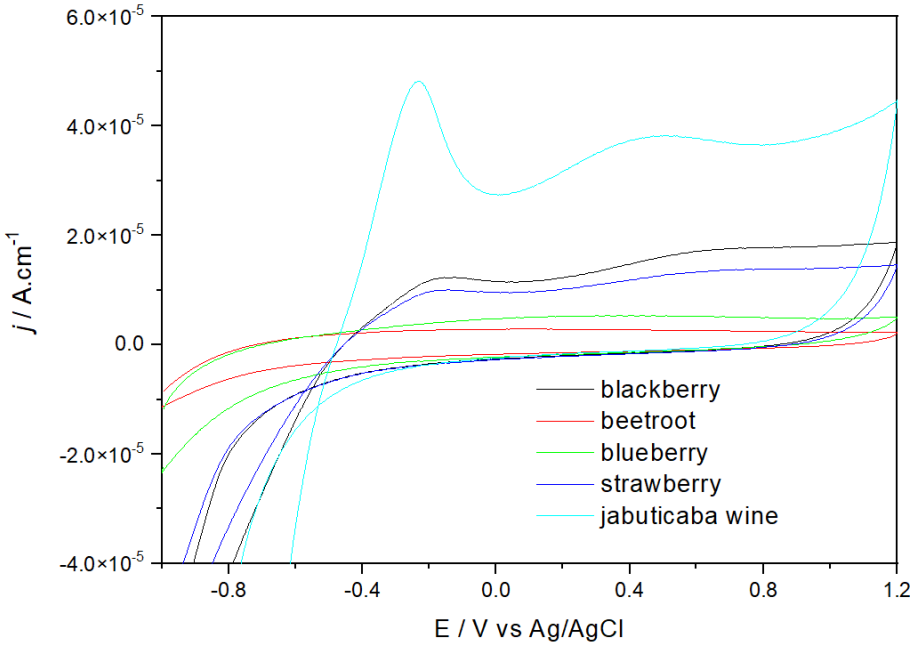

Figure 8. Cyclic voltammograms of ethanolic extracts of dyes.

Table 4. Anodic potentials of ethanolic extracts of dyes.

Dye extracts	**E_{ox} *vs* Ag/AgCl**
Blackberry	-0.157
Beetroot	-0.06
Blueberry	0.28
Strawberry	-0.185
Jabuticaba wine	-0.24

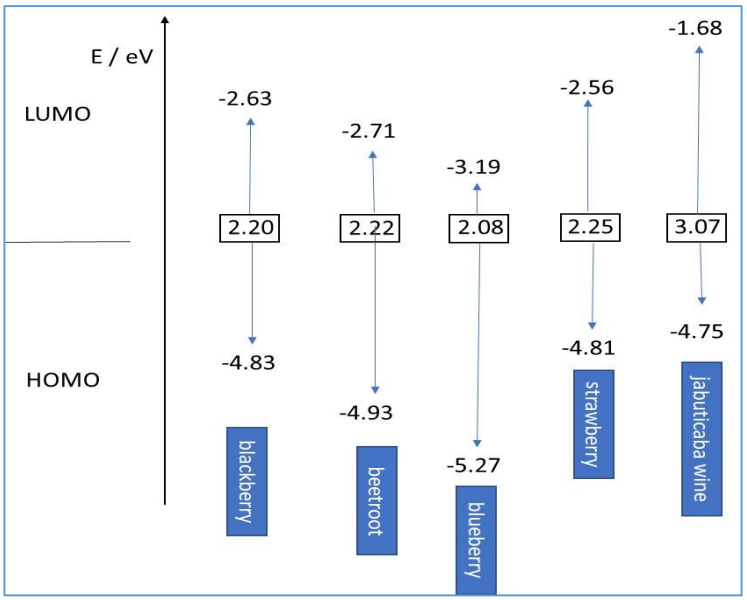

Figure 9. Diagram of the energy bands of ethanolic extracts of dyes with E_{gap} of the direct transition [19]**.**

3.4. Combination of components for its use in solar cell

Frequently, a DSSC contains a transparent conductive oxide as a substrate, such as PET/ITO, for the cathode or anode. The solar cell assembly can be completed with a semiconductor material such as VO_2 film that can be deposited onto PET/ITO, a sensitizer such as a natural dye coated onto the semiconductor followed by an electrolyte and a counter electrode on top such as PANI [20]. The energy levels of each component must be understood to assemble the best system for yielding the most efficient solar cell. Calculations were performed for each component variable (dye extract and PANI electrodeposition condition) to verify whether the combination of materials may result in a functioning and efficient solar cell. The combinations that were investigated are shown in Figure 10 together with a representation of the solar cell assembly. Subsequently, our group will prepare these combinations as well as their assembly to practically determine the best photovoltaic performance of these solar cells

1) VO_2/dye-blackberry extract/electrolyte/PANI (C1 or C2 or C3 or C4 or C6)
2) VO_2/dye-beetroot extract/electrolyte/PANI (C1, C2, C3, C4, or C6)
3) VO_2/dye-blueberry extract/electrolyte/PANI (all conditions)
4) VO_2/dye-strawberry extract/electrolyte/PANI (C1 or C2 or C3 or C4 or C6)
5) VO_2/dye-jabuticaba wine/electrolyte/PANI (C1 or C3 or C6)

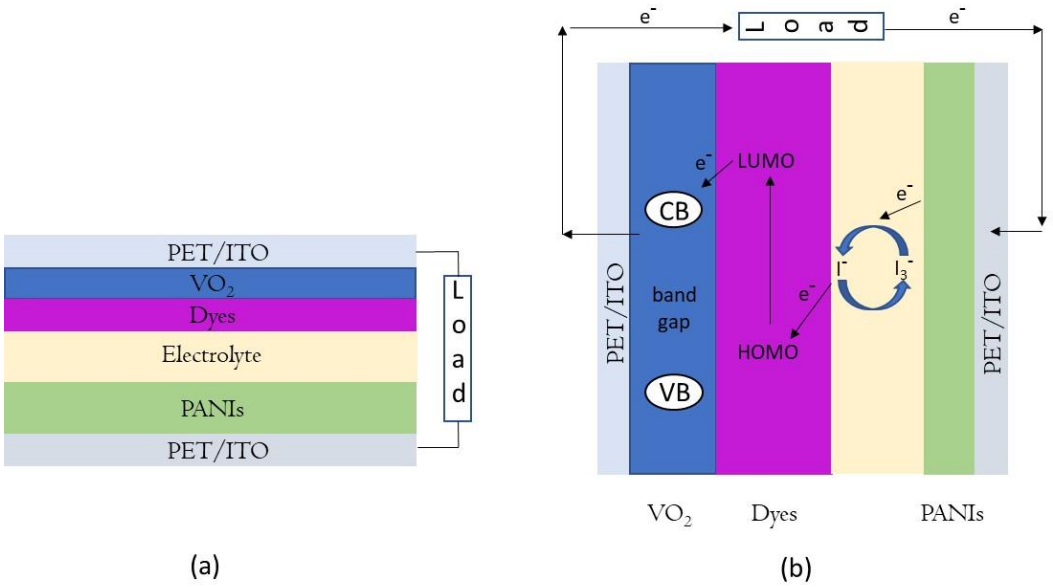

Figure 10. (a) Construction of DSSC, and (b) energy flow illustration.

4. CONCLUSIONS

The energy levels of electrodeposited PANI were influenced by changing the nature of the solution medium and the concentration of the monomer. VO_2 presented a band gap of 3.02 eV with HOMO and LUMO energy levels that were suitable for use as an anode in a DSSC. The extracted dyes from blueberry, blackberry, beetroot, jabuticaba wine, and strawberry have the ability to absorb visible light well and hence, have potential for use as the active donor material in DSSCs that utilize VO_2 as the semiconductor anode. The idea of this work was to find a good combination of cheap and easy to manufacture solar cells using natural dyes and PANI. After the full analysis and evaluation of each energy level of VO_2, the extracted dyes, and PANI, the next stage as to determine the efficiency of each combination. This was carried out to find a suitable new DSSC for industrial applications.

ACKNOWLEDGMENTS
This work was supported by INEO, FAPEMIG, RQ-MG/FAPEMIG, CNPq and CAPES.

References

1. F.H. Alharbi, S. Kais, *Renew. Sustain. Energy Rev.*, 43 (2015) 1073–1089.
2. A. Gusain, R.M. Faria, P.B. Miranda, *Front. Chem.*, 7 (2019).
3. F. Bendelala, A. Cheknane, H.S. Hilal, *Mater. Res. Express*, 5 (2018).
4. T.F.R. Shen, M.H. Lai, T.C.K. Yang, I.P. Fu, N.Y. Liang, W.T. Chen, *J. Taiwan Inst. Chem. Eng.*, 43 (2012) 95–101.
5. X. Liu, G. Xie, C. Huang, Q. Xu, Y. Zhang, Y. Luo, *Mater. Lett.*, 62 (2008) 1878–1880.
6. J.C. Valmalette, J.R. Gavarri, *Mater. Sci. Eng. B*, 54 B54 (1998) 168–173.
7. F. Guinneton, J.C. Valmalette, J.R. Gavarri, *Opt. Mater. (Amst).*, 15 (2000) 111–114.

8. H. Katzke, P. Tolédano, W. Depmeier, *Phys. Rev. B - Condens. Matter Mater. Phys.*, 68 (2003) 024109.
9. J. Schoiswohl, S. Surnev, F.P. Netzer, G. Kresse, *J. Phys. Condens. Matter*, 18 (2006) R1.
10. S.R. Takpire, S.A. Waghuley, *J. Mater. Sci. Mater. Electron.*, 27 (2016) 1007–1013.
11. C. Winder, N.S. Sariciftci, *J. Mater. Chem.*, 14 (2004) 1077–1086.
12. W. Li, L. Ye, S. Li, H. Yao, H. Ade, J. Hou, *Adv. Mater.*, 30 (2018) 1707170.
13. S.B. Kondawar, S.M. Pethe, *Adv. Mater. Lett.*, 5 (2014) 414–420.
14. B.L. da Silva, D.T. Cestarolli, E.M. Guerra, *J. Mater. Sci. Chem. Eng.*, 07 (2019) 12–23.
15. J.B. Coulter, D.P. Birnie, *Phys. Status Solidi Basic Res.*, 255 (2018) 1–7.
16. J. Tauc, Opt. Prop. Solids, Springer US, (1969) Boston, MA, pp. 123–136.
17. G. Brinker, CJ and Scherer, Sol-Gel Sci. - Phys. Chem. Sol-Gel Process., (1990) San Diego.
18. S. Wahyuningsih, L. Wulandari, M.W. Wartono, H. Munawaroh, A.H. Ramelan, *IOP Conf. Ser. Mater. Sci. Eng.*, 193 (2017).
19. A.. Maged, m. Amin, H. Osman, L.A.M. Nada, *Arab J. Nucl. Sci. Appl.*, 0 (2018) 0–0.
20. G. Richhariya, A. Kumar, *Opt. Mater. (Amst).*, 111 (2021) 110658.